Biodegradable and Functionally Superior Starch–Polyester Nanocomposites from Reactive Extrusion

Sathya Kalambur, Syed S. H. Rizvi

Department of Food Science, Cornell University, Ithaca, NY 14853

Received 16 January 2004; accepted 17 August 2004
DOI 10.1002/app.21504
Published online in Wiley InterScience (www.interscience.wiley.com).

ABSTRACT: Biodegradable starch-polyester polymer composites are useful in many applications ranging from numerous packaging end-uses to tissue engineering. However the amount of starch that can form composites with polyesters without significant property deterioration is typically less than 25% because of thermodynamic immiscibility between the two polymers. We have developed a reactive extrusion process in which high amounts of starch (approx. 40 wt%) can be blended with a biodegradable polyester (polycaprolactone, PCL) resulting in tough nanocomposite blends with elongational properties approaching that of 100% PCL. We hypothesize that starch was oxidized and then crosslinked with PCL in the presence of an oxidizing/crosslinking agent and modified montmorillonite (MMT) organoclay, thus compatibilizing the two polymers. Starch, PCL, plasticizer, MMT organoclay, oxidizing/crosslinking agent and catalysts were extruded in a co-rotating twin-screw extruder and injection molded at 120° C. Elongational properties of reactively extruded starch-PCL nanocomposite blends approached that of 100% PCL at 3 and 6 wt% organoclay. Strength and modulus remained the same as starch-PCL composites prepared from simple physical mixing without any crosslinking. X-ray diffraction results showed mainly intercalated flocculated behavior of clay at 1,3,6, and 9wt% organoclay. Scanning electron microscopy (SEM) showed that there was improved starch-PCL interfacial adhesion in reactively extruded blends with crosslinking than in starch-PCL composites without crosslinking. Dynamic mechanical analysis showed changes in primary α-transition temperatures for both the starch and PCL fractions, reflecting crosslinking changes in the nanocomposite blends at different organoclay contents. Also starch-polytetramethylene adipate-co-terephthalate (PAT) blends prepared by the above reactive extrusion process showed the same trend of elongational properties approaching that of 100% PAT. The reactive extrusion concept can be extended to other starch-PCL like polymer blends with polymers like polyvinyl alcohol on one side and polybutylene succinate, polyhydroxy butyrate-valerate and polylactic acid on the other to create cheap, novel and compatible biodegradable polymer blends with increased toughness. J Appl Polym Sci 96: 1072–1082, 2005

Key words: reactive extrusion; crosslinking; organoclay

INTRODUCTION

Even though the biodegradable polymer market has been active commercially for several years, it is in the initial stages of its product life cycle. The market for biodegradable polymers was approximately 20 million pounds in 2000 and is expected to be 60 million pounds by 2005.[1] Much of the increase in consumption is expected to come from polyesters such as polycaprolactone (PCL) and poly(lactic acid) (PLA) and their blends. A majority of the market share is expected to be in loose fill packaging, followed by compost bags, agricultural films, hygiene-related products, and paper coatings.[1] The two main factors that can increase the market scope and size of biodegradable polymers are cost and material properties. Incorporating starch into polyester matrices can lead to improvements in the stiffness, biodegradation kinetics, and final material cost.[2–4] These composites can also have net energy capacities comparable to those of fossil fuel-based plastics.[1] However, disadvantages associated with starch are as follows: (1) the immiscibility of native starch with all polyesters; (2) moisture absorption with time; and (3) the requirement of plasticizers, particularly for flexible material applications. Rather than a simple mixing of starch and polyesters, a reactive blend (RB) process is required to improve both the interfacial phase adhesion between the two polymers and the final material properties. In this article, *physical mixing* refers to composites and RBs blends to compatible blends prepared by reactive extrusion. Our group has recently developed an extrusion process that addresses this challenge through the reactive blending of starch and PCL.[5]

Starch is one of the major components of cereal grains. Corn and wheat are major sources of commercial starches in the United States. Other sources include rice, potatoes, peas, and tapioca. Starch is a mixture of two polysaccharides: amylose (linear 1,4-α-glucopyranosyl units) and amylopectin (linear 1,4-α-glucopyranosyl units and branched 1,6-α-glucopyr-

Correspondence to: S. Kalambur (sbk24@cornell.edu).

anosyl units).[6] The amylose fraction has a degree of polymerization (DP) of 1×10^2 to 4×10^5, and amylopectin has a DP of 1×10^4 to 4×10^7, with branches after every 19–25 linear units. Significant amounts of amylopectin (~75%) are present in most native corn and wheat starches, the rest being made up of amylose. However, commercially available corn starches have amylose contents varying from 0 (waxy maize) to approximately 70% (high amylose).[6] Therefore, blends made from different starches will have different properties based on the ratio of branched polymer fractions to linear polymer fractions in the blends.

Biodegradable polyesters that can form mechanically compatible composites with starch are PCL, poly(butylene succinate) (PBS), poly(tetramethylene adipate-*co*-terephthalate) (PAT), poly(hydroxy butyrate valerate) (PHBV), and PLA.[2,4,7–11] Many studies have been done on starch–PCL composites. Averous et al.,[2] Mani and Bhattacharya,[4] and Huang et al.[11] reported that the addition of starch to PCL caused an increase in the modulus by a factor of 1.5–3, a 50% decrease in the strength, and a very large decrease in the elongation to yield or break by a factor of 5–10. However, at 25 wt % amylose, PCL–amylose composites showed 5% less elongation at break, 10% less stress at break, and 20% less overall tensile strength than 100% PCL. Above 25 wt % amylose for PCL with a molecular weight of 80,000, the strength dropped off rather quickly, retaining less than one-half of its value at a 50 wt % amylose concentration. According to dynamic mechanical thermal analysis, amylose behaved as a phase-separated, low-particle-size filler for PCL. Studies done on starch–PHBV[12] composites also showed a decrease in the tensile strength upon the incorporation of starch. Starch was also found to affect biodegradation kinetics by increasing the rate over that of polyesters alone.[3–4] These studies[2,4,7–12] indicated that starch and polyesters were mechanically but not thermodynamically compatible, and significant property deterioration took place at starch concentrations greater than 25 wt %. In fact, starch–PCL composites and blends already exist in the market in various forms: MaterBi (composite) from Novamont SA (Novara, Italy),[9–10] Envar (RB) from Michigan State University (Lansing, MI),[13,14] and Bioplast (composite) from Biotech Corp. (Emmerich, Germany).[15] Significant market potential exists for starch-based biodegradable blends that can be used in the aforementioned applications.

To increase the amount of starch that can be incorporated into polyesters without property deterioration, small amounts of compatibilizers are needed. Until now, these compatibilizers have been produced in two ways: (1) the graft polymerization of a polyester monomer on the starch backbone and (2) the addition of various amounts of maleic anhydride (MA) modified polyester, which is added to a starch–polyester matrix to produce a compatibilized blend. Graft polymerization techniques have been used in starch–PCL blends,[7,13,14] and MA modifications have been done on starch blends with PCL, PHBV, PBS, and PAT.[4,16] For example, one of the commercially available starch–PCL products (Envar)[13,14] is synthesized by the first route. Narayan et al.[14] reported tensile properties of RB blown films synthesized by the polymerization of a caprolactone monomer on starch. At final concentrations of 70 wt % PCL and 30 wt % starch, the tensile strength showed an increase of 42%, but the elongation decreased by at least 59% over that of the control composite film. In another study, Choi et al.[7] reported that at starch/PCL ratios of 40:60, the tensile strength and modulus decreased with increasing amounts of grafted compatibilizers. However, the elongation increased eightfold over that of the composite at a 30 wt % compatibilizer concentration but was still 1/10 of the elongation of 100% PCL. They also found that grafted compatibilizers with short graft lengths and a high degree of graft polymerization were the most effective. Many studies have been done on the second route too. Mani and Bhattacharya[4] reported 3-fold and 1.5-fold increases in the tensile strength of starch–PCL and starch–PBS blends, respectively, with 50 wt % starch and 5 wt % MA modified polyester. However, no changes in the elongation or modulus were observed. No changes in the tensile properties of starch–PAT blends were reported. Similarly, Avella et al.[16] reported a threefold increase in the resilience of starch–PCL blends with 50 wt % starch and 10 wt % MA modified polyester as a compatibilizer. However, the resilience was still half that of 100% PCL. They also reactively blended starch with PHBV through the addition of organic peroxides. However, no property changes were reported. Thus, the graft polymerization and MA modification techniques do not work across the board for all polyesters,[4,7,13,16] and one property increase is offset by a decrease in another property. Also, these studies did not use plasticizers, and their effects on the reaction kinetics and overall properties were not evaluated.

Our research group has developed a reactive extrusion process in which starch is compatibilized with PCL in two steps but in a single extrusion process: (1) the partial oxidation of starch by the replacement of hydroxyl groups with carboxyls and carbonyls and (2) the crosslinking of oxidized starch with polyester by the abstraction of hydrogens near the carbonyl groups of oxidized starch and polyester.[5] Both these steps are performed through the addition of a single oxidizing/crosslinking agent and the generation of hydroxyl free radicals. Fenton's reagent (hydrogen peroxide with iron and copper catalysts) was used as the oxidizing/crosslinking agent. The crosslinking reaction was catalyzed by the addition of a modified high-surface-area montmorillonite (MMT) organoclay to ultimately produce tough starch–PCL nanocomposite RBs. A simplified reaction scheme is illustrated in Figure 1. Some of

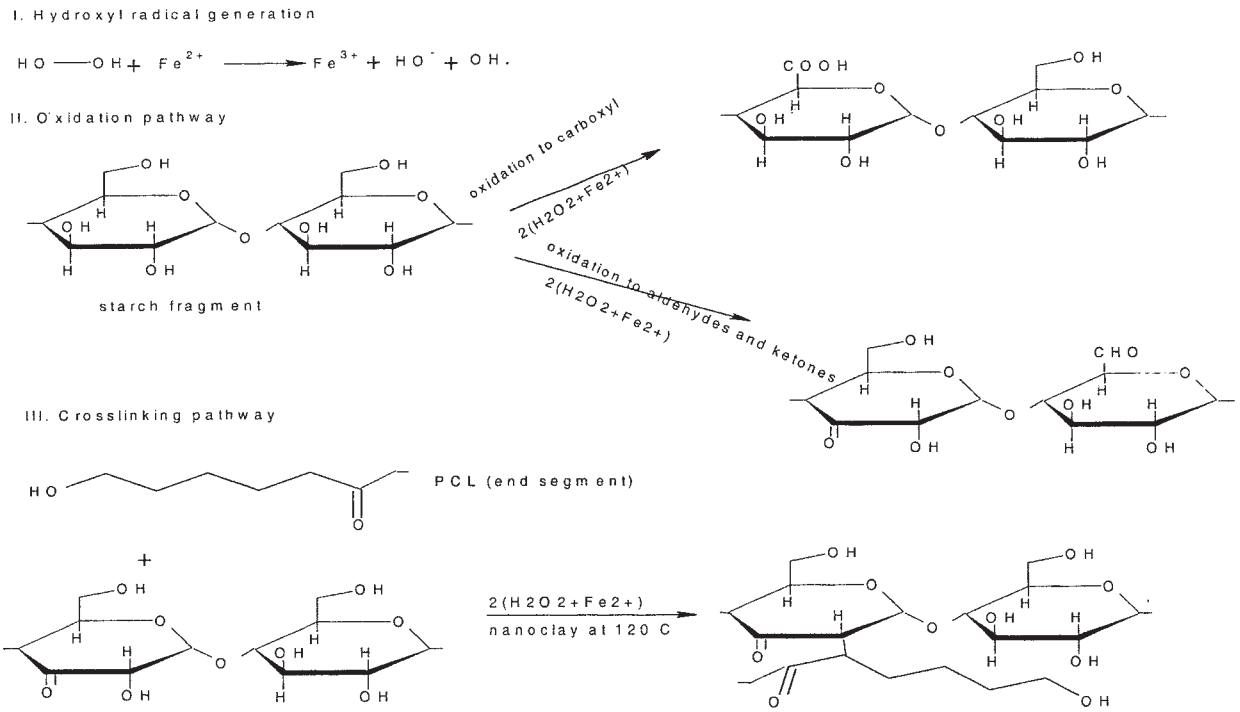

Figure 1 Simplified scheme of oxidation and crosslinking pathways.

the features of RBs produced in this manner are (1) greater toughness and elongation approaching that of 100% PCL and (2) improved interfacial adhesion between starch and PCL. This concept can be extend to other polymer blends with starch-like polymers, such as poly(vinyl alcohol) on one side and biodegradable and nonbiodegradable polyesters on the other.

EXPERIMENTAL

Native wheat starch (Midsol 50, Midwest Grain Products, Atchison, KS) had the following solid composition: 98.5% carbohydrates, 1% lipids, 0.2% proteins, and 0.22–0.25% ash. CAPA 6806 (Solvay Caprolactones, Warrington, England) is a PCL polymer with a number-average molecular weight of 80,000 (Lot #0871). Glycerol (Mallinckrodt, Hazelwood, MO) had at least 99.9% purity. Nanocor I.30E organoclay (Nanocor, Inc., Arlington Heights, IL) was an MMT type, with sodium ions (Na^+) replaced by quaternary ammonium octadecyl cations ($C_{18}H_{35}NH_4^+$). Hydrogen peroxide (30% solution in water; Fluka Cheme GmbH, Buchs, Switzerland) and ferrous and cupric sulfate catalysts (Fischer Scientific, Fairlawn, NJ) were constituents of Fenton's reagent. The formulations are given in Table I.

Reactive extrusion and injection molding

The ingredients were premixed and fed into a conical, corotating twin-screw microextruder (DACA Instruments, Goleta, CA). The residence time was kept at 3

TABLE I
Formulations Used in the Synthesis of Starch–PCL Nanocomposites by Reactive Extrusion

Code	Starch (%)	PCL (%)	Glycerol (%)	Organoclay (%)	H_2O_2 (mL/g of starch)[a]
STPCL	40	40	20	—	—
STPCLPERI-0	40	40	20	—	0.18
STPCLPERI-1	39.6	39.6	19.8	1	0.18
STPCLPERI-3	38.8	38.8	19.4	3	0.18[b]
STPCLPERI-6	37.6	37.6	18.8	6	0.18[b]
STPCLPERI-9	36.4	36.4	18.2	9	0.18[b]

[a] 30% solution in water; ferrous and cupric sulfate catalysts were used at 0.0025 and 0.002 g/g of starch on a wet basis.
[b] Two other levels of peroxide were also used, 0.27 (level II) and 0.36 mL/g of (level starch (level III), as indicated by STPCLPERII and STPCLPERIII, respectively.

min, and the melt was then extruded out of the die in the form of cylindrical strands. The temperature throughout the extruder was kept at 120°C, and the screw speed was kept at 115–120 rpm. The extruder barrel was blanketed with nitrogen during extrusion. Two batches of each formulation were extruded to ensure reproducibility. The extruded strands were injection-molded into a microinjector (DACA Instruments) in the form of dog-bone pieces. The barrel was kept at 120°C, and the mold was kept at the ambient temperature.

Tensile properties

Tensile measurements of dog-bone pieces were performed on an Instron 1122 universal tester (Instron Corp., Canton, MA) at a crosshead speed of 50 mm/min. The maximum stress, elongation at rupture, and Young's modulus were measured. The modulus was calculated by a regression analysis of the stress–strain data up to a 1% strain.

Scanning electron microscopy (SEM)

SEM was used to analyze the domain structure of the starch phase in the starch–PCL composites and nanocomposite blends. Molded samples were ultrasonicated for 5 min in warm water at 40°C. The samples were then analyzed with a Leica 440 scanning electron microscope (Leica Microsystems Inc., Bannockburn, IL) at an electric field strength of 10 kV.

X-ray diffraction

The clay dispersion behavior was studied by X-ray diffraction (Scintag θ–θ wide-angle X-ray diffractor working at 40 kV and 30 mA). Flat, molded samples were used for the diffraction analysis.

Thermal properties: differential scanning calorimetry (DSC)

Molded samples were analyzed by DSC (DSC 2920, TA Instruments, New Castle, DE) to determine the PCL crystal properties. Approximately 3–10 mg of each molded sample was placed in an aluminum pan, which was then sealed. For crystallization experiments, the sample was rapidly heated to 120°C and equilibrated for 3 min. Then, it was cooled to 0°C at a rate of 10°C/min. For melting and crystallinity experiments, the samples were rapidly heated to 120°C, equilibrated for 3 min, quenched to 0°C, held for 3 min, and heated to 120°C at 10°C/min. The maxima of the melting endothermic and exothermic crystallization peaks were taken as the melting temperature (T_m) and crystallization temperature (T_c), respectively, and the melting peak areas were used to calculate the enthalpy of fusion and crystallinity. The peak areas were measured from the flat baseline on one side and the maximum change in the curved baseline slope on the other. The crystallinity percentage (X_c) of the PCL component in the composites and RB nanocomposites was obtained as follows:

$$X_c = \Delta H_f / (w \times \Delta H_{f,100\%})$$

where $\Delta H_{f,100\%}$ and ΔH_f are the heats of fusion for 100% crystalline PCL and PCL, respectively, and w is the weight fraction of PCL. $\Delta H_{f,100\%}$ was taken to be 142 J/g.[17]

TABLE II
Tensile Properties of Starch–PCL Blends and Reactively Extruded Nanocomposites

Sample	Maximum strength (MPa)	Young's modulus (MPa)	Elongation at break (%)
100% PCL	35.7	13.0	1101.9
	(0.6)	(0.4)	(22.0)
STPCL	12.6	19.4	246.6
	(1.2)	(0.6)	(15.0)
STPCLPERI-0	3.2	7.1	199.6
	(0.8)	(1.2)	(18.2)
STPCLPERI-1	8.6	11.6	568.1
	(0.3)	(0.7)	(35.8)
STPCLPERI-3	10.2	15.6	926.0
	(0.4)	(0.6)	(22.0)
STPCLPERI-6	10.0	18.6	877.0
	(0.3)	(0.6)	(24.8)
STPCLPERI-9	9.5	21.1	672.0
	(0.3)	(1.0)	(31.5)

The values in parentheses are standard deviations.

Dynamic mechanical analysis (DMA)

Dynamic viscoelastic properties of molded nanocomposites were measured with a PerkinElmer DMA 7e (PerkinElmer Instruments, Shelton, CT). Molded samples ($1.5 \times 4.0 \times 10$ mm^3) were analyzed in the three-point bending mode. The storage modulus, loss modulus, and phase-angle shift were measured at a frequency of 1.6 Hz and at a scanning rate of 4°/min from −120 to 52°C.

Carbonyl and carboxyl concentrations in the oxidized starch

Carboxyl determination

A dry sample (~1 g) was slurried in water (100 mL), and 0.975*M* NaOH was added to keep the pH above 10. After 1 h of stirring, the mixture was back-titrated with 0.118*M* HCl to the phenolphthalein endpoint (pH 8.3). Composites with no peroxide were used as controls.

Carbonyl determination

A dry sample (~1 g) was slurried in water (300 mL) and heated to boiling to completely solubilize it. The cooled solution was adjusted to pH 3.2 with 0.118*M* HCl, and 60.0 mL of a hydroxylamine hydrochloride (25 g) solution was added (100 mL of 0.5*M* NaOH diluted to 500 mL). The solution was heated to 40°C in an oven for 4 h and titrated rapidly to pH 3.2 with 0.118*M* HCl. A water sample was used as a control:

$$\% \text{ C}{=}0 = 0.118 \times 0.028 \times [\text{Control(mL)} - \text{Sample(mL)}] \times 100$$

RESULTS AND DISCUSSION

Tensile properties

The tensile properties of the starch–PCL composites and nanocomposite blends are given in Table II. In comparison with 100% PCL, the addition of starch at a ratio of 1:1 with PCL reduced the strength and elongation by more than 50% in the STPCL composites, whereas the modulus increased slightly over that of 100% polyester. The increase in the modulus upon the addition of starch to PCL has been observed in other studies.[2,4,11] Starch, being a more rigid polymer than PCL, contributed to higher stiffness. As shown in DMA studies, the α primary transition of PCL was lower (~−57°C) than that of starch (~4°C) in the STPCL composites.

Compared with that of the STPCL composites, the elongation was dramatically improved in the RB nanocomposites. At 3 and 6 wt % organoclay concentrations, the elongation approached that of 100% PCL. The elongation at break reached a maximum at 3 and 6% organoclay concentrations and went down at a 9% organoclay concentration. The increase in the elongation can be attributed to better interfacial adhesion between the starch and PCL. Better interfacial adhesion was similarly associated with improved elongation in an RB study by Choi et al.[7] As shown in Figure 1, during the RB extrusion process, a small amount of crosslinked species was formed. This could include starch–starch, PCL–PCL, and starch–PCL crosslinks. However, only starch–PCL crosslinks were expected to improve starch–PCL interfacial adhesion, whereas intramolecular crosslinks would reduce it.[11] The tensile results indicated that starch–PCL crosslinks might have predominated instead of the other types of crosslinks. Also, glycerol might have played an important role in crosslinking. It is not known yet if there exists a system in which starch, PCL, and glycerol are crosslinked together and, if so, how much crosslinking is present.

In the RB nanocomposites with 6 and 9% clay concentrations, the strength and modulus approached

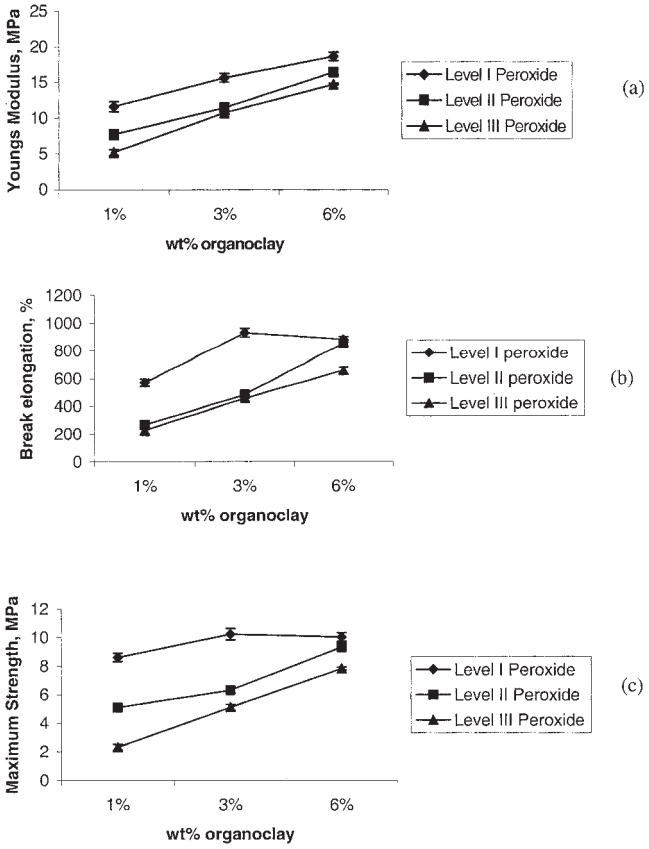

Figure 2 Effect of clay and peroxide levels on (a) Young's modulus, (b) elongation at break, and (c) maximum strength. Levels I, II, and III had 0.18, 0.27, and 0.36 mL of peroxide/g of starch, respectively.

and surpassed, respectively, that of STPCL composites. Within the RB nanocomposites, no large differences in the maximum strength were observed, but the modulus increased as the clay concentration increased. This was due to a reinforcement effect from the dispersion of the organoclay in the starch–PCL matrix through mechanisms described elsewhere.[18] Also, reactively extruded starch–PCL blends without any organoclay (STPCLPERI-0) showed poor properties. We hypothesize that the organoclay affected the crosslinking dynamics in the following manner. In the STPCLPERI-0 sample, crosslinking was expected to be more extensive than in starch–PCL nanocomposites. However, the addition of the organoclay resulted in decreased and optimum crosslinking density because the clay sheets were expected to act as a physical barrier to crosslinking. The exact mechanism of how organoclay affects crosslinking kinetics is not known yet. It may be that in STPCLPERI-0, crosslinking could be more intramolecular than intermolecular. As discussed later, DSC and DMA results reflected crosslinking changes between STPCLPERI-0 and other nanocomposites.

In summary, we have developed a reactive extrusion process to produce starch–PCL polymer blends

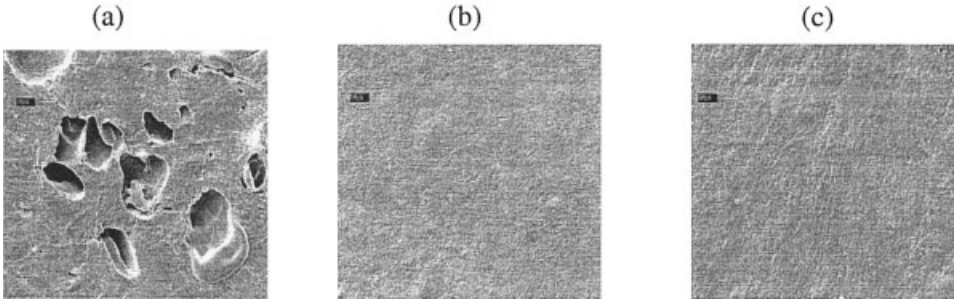

Figure 3 SEM pictures of ultrasonicated samples: (a) STPCL, (b) STPCLPERI-3, and (c) STPCLPERI-6. From left to right, there is increasing interfacial adhesion between starch and PCL.

tougher than what exists in the market today (Mater-Bi from Novamont and Envar from Michigan State University). This concept can be extended to different types of polymers containing hydroxyl groups and to different types of polyesters (biodegradable and nonbiodegradable) to tailor RB nanocomposites with application-specific properties. For example, starch–PAT (Eastar Bio Ultra, Eastar Chemicals, Sacramento, CA) nanocomposites prepared by the same reactive extrusion procedure also followed the same trend in the tensile properties, with an almost fivefold increase in the elongation over that of starch/Eastar Bio composites (results not shown).

Effect of the peroxide level

The tensile properties of RB nanocomposites containing three different levels of peroxide are shown in Figure 2. Levels I, II, and III contained 0.18, 0.27, and 0.36 mL of peroxide/g of starch, respectively. As shown in Figure 2, the best properties were obtained at the peroxide level of 0.18 mL/g of starch. The differences in the properties at the different peroxide levels can be explained in two ways: (1) the depolymerization of starch/PCL molecule by hydrolysis at higher peroxide levels (levels II and III) and (2) changes in the density of starch–PCL crosslinks at different peroxide levels. Other studies have indicated that significant depolymerization of starch takes place in the presence of oxidizing agents.[19–21] Wing and Willett,[19] using a starch oxidation method similar to that used in this study, found that with level I peroxide, the apparent viscosities of 5% solutions (in water) of oxidized starches were comparable to those of maltodextrins with a dextrose equivalent of 5–10. In the RB nanocomposites with level I peroxide, however, as the tensile property data showed and as the DMA results will show later, the depolymerization did not adversely affect the mechanical properties and did not affect the primary polymer (starch and PCL) relaxations.

Morphology

SEM pictures of STPCL, STPCLPERI-3, and STPCLPERI-6 are shown in Figure 3. The pictures were ob-

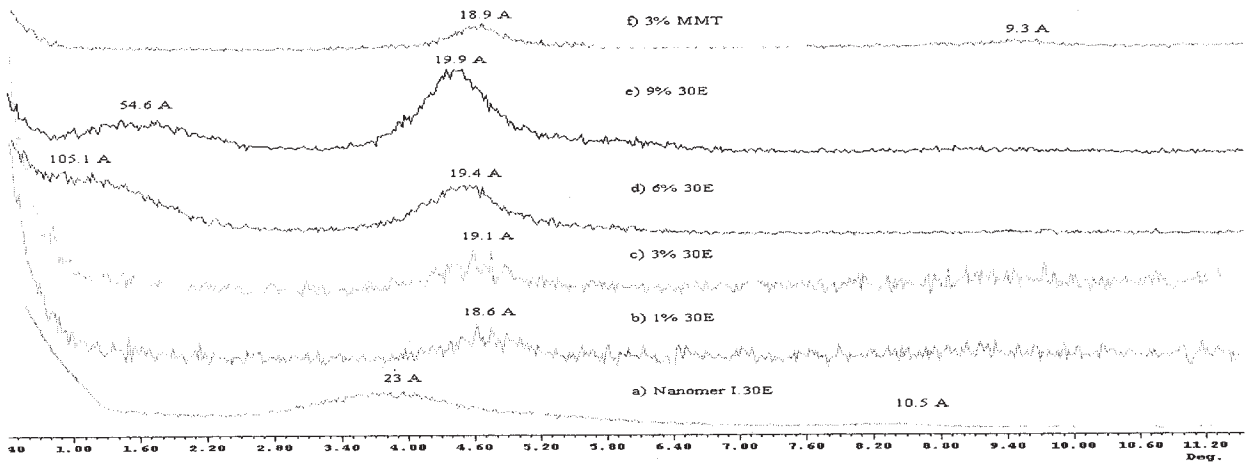

Figure 4 X-ray diffraction spectra of (a) nanomer 1.30E with a *d*-spacing of 23 Å, (b) 1% nanomer I.30E in a starch–PCL nanocomposite, (c) 3% nanomer I.30E in a starch–PCL nanocomposite, (d) 6% nanomer I.30E in a starch–PCL nanocomposite, (e) 9% nanomer I.30E in a starch–PCL nanocomposite, and (f) 3% MMT clay in a starch–PCL blend.

TABLE III
Melting and Crystallization Properties of Starch–PCL Composites and Blends

Material	T_c (°C)	T_m (°C)	X_c (%)	Relative crystallinity
100% PCL	27.40[a]	57.59[a]	30.10[a]	1.00[a]
STPCL	26.71[b]	55.71[b]	32.17[a]	1.07[a]
STPCLPERI-0	21.47[c]	54.32[c]	26.05[b]	0.87[b]
STPCLPERI-1	20.77[c]	54.18[c]	27.10[b]	0.90[b]
STPCLPERI-3	22.57[d]	55.50[b,d]	28.85[a,c]	0.96[a,c]
STPCLPERI-6	23.60[e]	55.00[b,d]	29.71[a,c]	0.99[a,c]
STPCLPERI-9	24.01[e]	54.92[d]	30.37[a,c]	1.01[a,c]

Number of replicates = 6. The same superscript letters indicate the same mean, and different letters indicate a significant difference at $\alpha = 0.05$ by a t test for independent means.

tained from molded samples that were ultrasonicated in water for 5 min at 40°C. The pictures were magnified 2000×. Even though starch is a hydrophilic polymer, it is not possible to etch the polymer by immersion in water. Ultrasonication aids in the etching process of hydrophilic starch from its domain in the starch–PCL polymer matrix into surrounding water. As shown in Figure 3, STPCL had large voids in place of starch, whereas STPCLPERI-3 and STPCLPERI-6 had no voids. Starch in STPCL composites was immiscible with PCL, as expected, and showed easy separation from its domains. However, in the RB nanocomposites with the organoclay, there was better interfacial adhesion, which resulted in no phase separation of starch upon ultrasonication. Choi et al.[7] observed similar results for starch–PCL blends compatibilized with a starch-grafted PCL copolymer. In this study, the improved interfacial adhesion came from intermolecular starch–PCL crosslinked species that acted as a compatibilizer between uncrosslinked starch and PCL.

Dispersion of the organoclay

Figure 4(a) shows the diffraction spectra of 100% nanomer I.30E clay. There were two peaks, the larger one with a d(001) spacing of 23 Å and a smaller one with a spacing of 10.5 Å. Through the integration of the areas, we found that approximately 5–6% of the nanomer 30E organoclay was unmodified clay or a natural MMT clay. Figure 4(b–e) shows the spectra of 1, 3, 6, and 9 wt % clay RB nanocomposites. There was one peak at 18.6–19.9 Å that increased in intensity with increasing clay content. Also, there were additional peaks in the 6 and 9% clay spectra. The peak for the 6% clay had a d-spacing of 105.1 Å, although it was not completely resolved and appeared as a shoulder. At a 9% clay concentration, a distinct peak could be seen at 54.6 Å. Figure 4(f) shows the spectra of 3% MMT (unmodified nanoclay) RB nanocomposites. There were two d-spacings, one at 18.9 Å showing intercalation and a smaller one at 9.3 Å indicating that a small fraction of the MMT clay was still present as agglomerated sheets. However, the peak corresponding to agglomerated sheets was not seen in the RB nanocomposites containing nanomer 30E organoclay. These data show that the organoclay was intercalated and flocculated, and increased flocculation was observed as we increased the modified clay content from 1 to 9%. At a 6% clay concentration, there seemed to be intercalation at 105.1 Å. This peak shifted to 54.6 Å at a 9% clay concentration. The presence of a peak at 18.6–19.9 Å in the RB nanocomposites with modified clay could be due to two reasons: (1) the d-spacing of an unmodified fraction of the organoclay increased from 10.5 Å, or (2) some of the alkyl ammonium cations in the organoclay were leached out during the peroxide oxidation process. This seemed more likely because the d-spacing of this peak was similar to that of the unmodified clay nanocomposite [Fig. 4(f)]. Additional transmission electron microscopy studies will be performed to ascertain this.

Thermal properties

The PCL crystallization and T_m variations in the starch–PCL composites and nanocomposite RBs are illustrated in Table III. T_c of the RB nanocomposites increased between 1 and 9% organoclay concentrations in comparison with that of STPCLPERI-0 but remained lower than that of STPCL composites and 100% PCL. A large number of PCL crosslinking sites in the STPCLPERI-0 sample reduced the mobility of the polymer chain and hindered its ability to crystallize.[11] Thus, STPCLPERI-0 had a lower T_c than STPCL and 100% PCL. T_c differences within the RB nanocomposites could be due to combination of two factors:

1. Differences in the crosslinking densities at different organoclay contents, with higher crosslinking leading to lower T_c. Higher crosslinking hindered the structural relaxations of the polymer molecules required for crystallization.[11]
2. Organoclay layers acting as nucleating agents and causing a crystallization rate higher than that of STPCLPERI-0.[22] However, the effective increase from nucleation could be offset by a

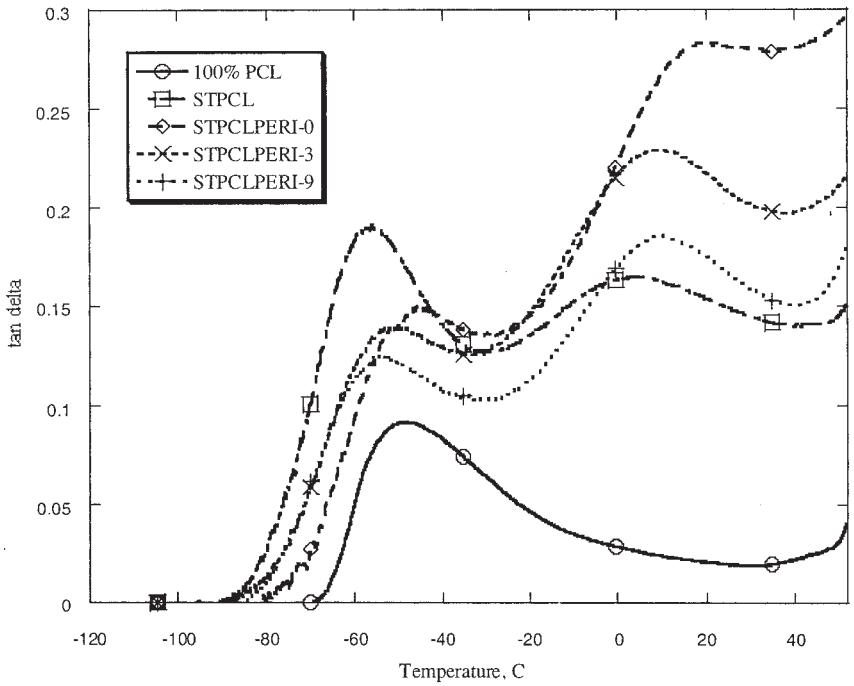

Figure 5 Tan δ peaks of starch–PCL blends. Each curve is the average of five to six replicates.

greater number of interactions between the PCL and organoclay. These interactions affected the crystallization kinetics by hindering entropic changes that normally occurred during crystallization.[23] Thus, overall the net increase in T_c of the RB nanocomposite samples, compared with that of STPCLPERI-0, was not very large, as observed for other PCL–organoclay systems.[22,23]

T_m of the STPCL composites decreased slightly over that of 100% PCL. This could be attributed to a dilution and limited plasticizing effect arising from the presence of both starch and glycerol. However, no large changes were found in the RB samples with respect to STPCL. This indicated that there were few changes in the crystal type or size of the crystal in the presence of the organoclay and reactive extrusion. Also, no other endothermic peaks were observed up to 120°C. This suggested that most of the starch was destructurized, and the starch crystalline phase was lost.

PCL crystallinity in STPCLPERI-0 decreased significantly over that of STPCL and 100% PCL. Extensive crosslinking in STPCLPERI-0 could lead to a crystallinity decrease, and this phenomenon has been observed in other crosslinked PCL systems.[7,11] However, the crystallinity increased with increasing organoclay content and achieved the same level as that of STPCL with 3, 6, and 9% organoclay concentrations. This indicated that crosslinking density differences in the nanocomposite systems with 3, 6, and 9 wt % organoclay could not be statistically resolved with DSC. Also, the increased crystallinity in the RB nanocomposites could be associated with decreased crosslinking density in the presence of the organoclay. Thus, significant improvements in the tensile elongation were achieved from small amounts of starch–PCL crosslinking, and the changes in the mechanical properties were not due to changes in the PCL crystalline morphology. Similar amounts of PCL crystallinity in the STPCL and RB nanocomposites with 3, 6, and 9 wt % organoclay implied small amounts of crosslinking in them in comparison with uncrosslinked PCL in STPCL composites. This had relevance to the biodegradation rate too, as highly crosslinked PCL showed reduced biodegradation rates in other studies.[3,11]

Dynamic mechanical properties

Figure 5 shows tan δ peaks of 100% PCL, starch–PCL composites, and RB nanocomposite blends. The observed salient features were as follows:

1. Two α transitions in the STPCL composites, corresponding to starch and PCL.
2. An increase in the maximum/peak value of a damping peak ($(\tan \delta)_{max}$) of the PCL peak in STPCL over that of 100% PCL.
3. A decrease in $(\tan \delta)_{max}$ of PCL and an increase in $(\tan \delta)_{max}$ of starch peaks in STPCLPERI-0 in comparison with those in STPCL.

TABLE IV
Damping behavior of Starch–PCL Blends

Material	$T_{\alpha 1}$ (°C)	$(\tan \delta 1)_{max}$	$T_{\alpha 2}$ (°C)	$(\tan \delta 2)_{max}$	Half peak width of starch relaxation (°C)
100% PCL	−51	0.092	—	—	—
STPCL	−57	0.191	4	0.164	29.9
STPCLPERI-0	−47	0.149	18	0.283	ND
STPCLPERI-1	−49	0.144	15	0.234	22.6
STPCLPERI-3	−51	0.139	10	0.223	22.5
STPCLPERI-6	−51	0.124	11	0.194	23.9
STPCLPERI-9	−54	0.124	10	0.185	24.7

Number of replicates = 5–6. ND = could not be determined. $T_{\alpha 1}$ and $T_{\alpha 2}$ are the α-transition temperatures of PCL and starch, respectively, and were measured at their peak maximum.

4. A decrease in $(\tan \delta)_{max}$ of PCL and a decrease in $(\tan \delta)_{max}$ of starch peaks with an increasing organoclay concentration.
5. Changes in the α-transition temperatures of PCL and starch fractions within the RB nanocomposites.

Table IV shows changes in the α transition and peak damping values of 100% PCL, starch–PCL composites, and RB nanocomposites. In STPCL, the transition of starch was broader than that of PCL because the amylopectin fraction of the native starch was highly branched. This led to a wide distribution of transition temperatures of starch corresponding to each population of starch molecules with different branching lengths and densities. In the presence of starch in the STPCL samples, the PCL α transition decreased. This could be attributed to a limited plasticizing effect of both glycerol and starch in the blend. This plasticizing effect also contributed to a small change in the PCL T_m, as observed from DSC results listed in Table III. The $(\tan \delta)_{max}$ value of the PCL peak in STPCL increased over that of 100% PCL. A small part of this increase could be attributed to the increasing mobility of PCL molecules due to the plasticizing effect of starch and glycerol, even though the PCL crystallinity remained the same in 100% PCL and STPCL samples. Also, other studies have shown secondary β transitions for starch–glycerol mixtures in the α-transition region of PCL.[2,24] This could have led to a superimposition effect and thus greatly increased the peak damping values in the PCL transition region.

RB samples, both with and without the organoclay, showed increases in the α-transition temperatures for both polymeric components: starch and PCL. As illustrated in Table IV, α transitions for STPCLPERI-0 showed the highest increase over that of STPCL. The transitions showed a decreasing trend with an increasing organoclay level. However, even with 9 wt % organoclay, the transitions were still higher than those in STPCL. The changes in the α-transition temperatures could be attributed to the following factors:

1. Comparing STPCL and STPCLPERI-0, the increase in the polymer transition temperatures could be associated with crosslinking and copolymerization effects.[25] The increase in the transition temperatures indicated that crosslinking predominated instead of starch depolymerization, which would reduce the transition temperature. Thus, even though starch depolymerization was observed in a similar starch oxidation study by Wing and Willett,[19] this did not affect the starch transition temperature.
2. Within the RB nanocomposites, the transition temperature of starch and PCL decreased with an increasing organoclay concentration. One reason could be that the density of crosslinking decreased with an increasing organoclay concentration. The organoclay, because of its high aspect ratio and surface area, was expected to act as a significant physical barrier to crosslinking. Also, the decrease in the α transition with an increasing clay concentration could not be associated with depolymerization effects because complex viscosity curves (data not shown) showed increasing viscosity with an increasing organoclay level. The second reason could be that increased intercalation of PCL and starch with an increasing organoclay concentration could reduce the transition temperature. Similar decreases in the glass transitions of crosslinked

TABLE V
Oxidation Levels of Starch in Starch–PCL RBs

Material	—COOH (mmol/g)	—C═O (%)
STPCLPERI-0	1.01[a]	6.3[a]
STPCLPERI-3	0.55[b]	6.7[a]
STPCLPERI-6	0.15[c]	4.3[b]
STPCLPERI-9	0.16[c]	5.1[b]

Number of replicates = 3–4. The same superscript letters indicate the same mean, and different letters indicate a significant difference at $\alpha = 0.05$ by a t test for independent means.

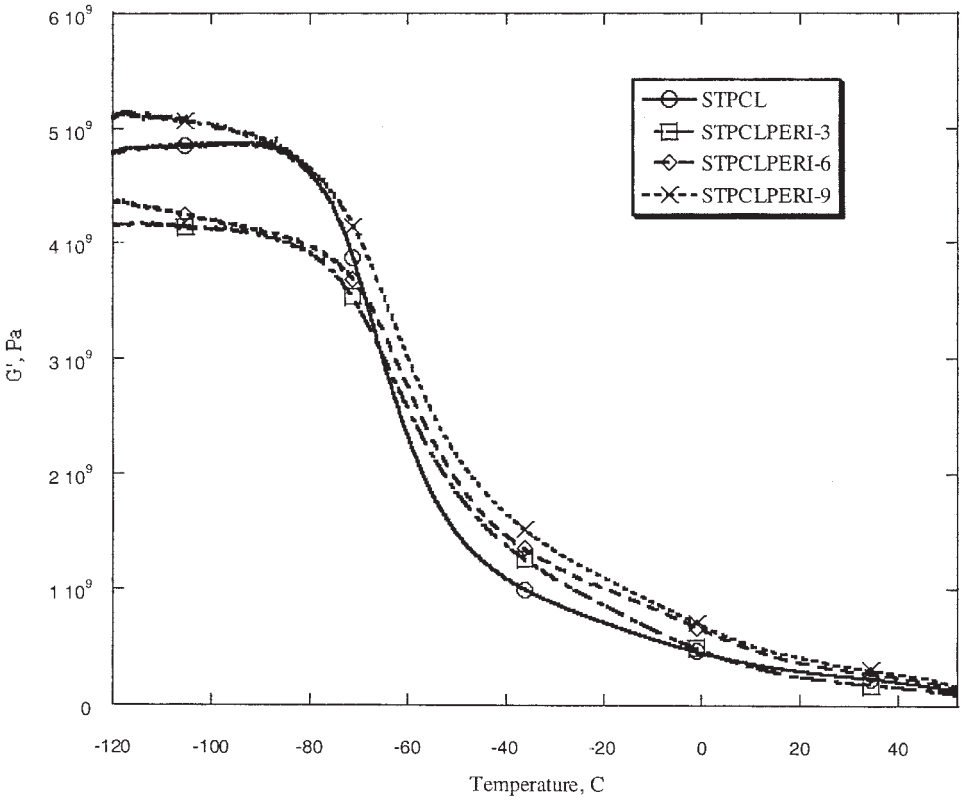

Figure 6 Storage modulus (G') of STPCL and RB nanocomposites at 3, 6, and 9 wt % organoclay concentrations. Each curve is the average of five to six replicates.

epoxy nanocomposite systems have been reported in other studies.[26,27] The decrease indicated that the polymer chains were not tied down on the surfaces of the silicates. However, because this polymer system was affected by starch oxidation, crosslinking and polymer–organoclay interactions, the changes observed could be due to a combination of these three factors.

In comparison with STPCL, STPCLPERI-0 showed interesting damping behavior. A decrease in $(\tan \delta)_{max}$ of the PCL peak could be attributed to increased crosslinking and a smaller fraction of amorphous PCL. The oxidation of starch led to a very high $(\tan \delta)_{max}$ value for the starch peak in STPCLPERI-0. However, the starch peak was very broad compared with those for STPCL and even RB nanocomposites. The near disappearance of the starch peak was consistent with very high crosslinking in STPCLPERI-0.

Table V lists starch oxidation levels at different organoclay levels. The addition of 3 wt % organoclay reduced the carboxyl content, whereas the carbonyl content was the same. With 6 and 9 wt % organoclay, both the carboxyl and carbonyl contents decreased further, and this indicated lower oxidation. Under the reaction conditions, more carbonyls than carboxyls were formed than reported in a similar starch oxidation study.[19] This could be due to the easy accessibility of hydroxyl groups in H_2O_2 due to the ease of starch gelatinization in the presence of glycerol and at elevated temperatures. The decrease in $(\tan \delta)_{max}$ of the starch peak in the RB nanocomposites, compared with that for STPCLPERI-0, was accompanied by decreased overall oxidation of the starch. The $(\tan \delta)_{max}$ value of the PCL peak in the RB nanocomposites also decreased with an increasing organoclay concentration. This change in the PCL damping peak was likely caused by crystallinity differences, even though these could not be statistically resolved with DSC for nanocomposites with 3, 6, and 9 wt % organoclay. The decreases in $(\tan \delta)_{max}$ for starch and PCL with an increasing clay concentration could also be attributed to strong polymer–clay interactions. Weaker interactions and the agglomeration of organoclay sheets have been known to increase damping because of higher friction between the polymer and organoclay particles, whereas strong interactions reduce damping.[28,29] Thus, the overall damping of the starch fraction was affected more by oxidation and polymer–clay interactions than by crosslinking, which tended to reduce damping, whereas that of the PCL fraction seemed to be affected by crosslinking and polymer–clay interactions. The starch α-relaxation peak half-widths of the

STPCL composite and RB nanocomposites are shown in Table IV. The widths of the RB nanocomposites showed a significant reduction over that of STPCL. This could not be caused by the organoclay because unfilled systems such as STPCL are generally less broad than filled systems.[30] The decrease in the peak widths of the RB nanocomposites could explain the improved elongational properties to some extent. The broadening of the α transition might be related to restrained chain mobility making molecular relaxations more difficult.[31] This implied greater intermolecular slippage in the nanocomposite RBs before final rupture than in STPCL. The half-widths of the PCL peaks could not be measured because the damping increased with increasing temperature before the whole peak was formed.

Figure 6 shows the storage modulus curves for the STPCL composite and RB nanocomposites with 3, 6, and 9 wt % organoclay. The storage modulus increased as the organoclay concentration increased in all regions. However, the increases were small in comparison with those found for uncrosslinked PCL–organoclay systems.[23,32] The increase in the storage modulus with an increasing organoclay concentration was offset by a decreasing crosslinking density, as shown by the α-transition changes. Thus, the overall increase was smaller than expected. Also, in the glass–rubbery transition region, the storage modulus of the RB nanocomposites was higher than that of STPCL. However, near the ambient temperature in the plateau region, the storage modulus of STPCL was higher than that of STPCLPERI-3 and STPCLPERI-6 but lower than that of STPCLPERI-9. This was analogous to the tensile modulus results shown in Table II.

CONCLUSIONS

A new reactive extrusion chemistry was developed to improve interfacial adhesion between starch and PCL. Fenton's reagent was used to oxidize starch and initiate crosslinking between oxidized starch and PCL. The crosslinking step was catalyzed by an MMT organoclay with a high surface area and aspect ratio. The elongation of these nanocomposites was comparable to that of 100% polyester. The strength and modulus remained the same as those in starch–PCL composites without crosslinking. This reactive extrusion process could be extended to other starch–PCL-like polymer blends with polymers such as poly(vinyl alcohol) on the one side and PBS, PHBV, and PLA on the other to create cheap, novel, and compatible biodegradable polymer blends with increased toughness.

The authors thank Prof. E. Giannelis at the Department of Materials Science, Cornell University, for use of the microextrusion and injection-molding facilities.

References

1. Gemgross, T. U.; Slater, S. C. Sci Am 2000, 283, 37.
2. Averous, L.; Moro, L.; Dole, P.; Fringant, C. Polymer 2000, 41, 4157.
3. Tokiwa, Y.; Iwamoto, A.; Koyama, M. Polym Prepr 1990, 63, 742.
4. Mani, R.; Bhattacharya, M. Eur Polym J 2001, 37, 515.
5. Kalambur, S.; Rizvi, S. S. H. Polym Int, 2004, 53, 1413.
6. Kaplan, D. L.; Mayer, J. M.; Ball, D.; McCassie, J.; Alien, A. L.; Stenhouse, P. In Biodegradable Polymers and Packaging; Ching, C.; Kaplan, D.; Thomas, E., Eds.; Technomic: Lancaster, PA, 1993; p 1.
7. Choi, E. J.; Kim, C. H.; Park, J. K. J Polym Sci Part B: Polym Phys 1999, 37, 2430.
8. Willett, J. L.; Shogren, R. L. Polymer 2002, 43, 5935.
9. Bastioli, C.; Bellotti, V.; Del Tredici, G.; Guanella, I.; Lombi, R. U.S. Pat. 6,348,524 (1999).
10. Bastioli, C.; Raffa, G.; Rallis, A. U.S. Pat. 5,902,262 (1995).
11. Huang, S. J.; Koenig, M. F.; Huang, M. In Biodegradable Polymers and Packaging; Ching, C.; Kaplan, D.; Thomas, E., Eds.; Technomic: Lancaster, PA, 1993; p 97.
12. Ramsay, B. A.; Langlade, V.; Carreau, P. J.; Ramsay, J. A. Appl Environ Microbiol 1992, 59, 294.
13. Dubois, P.; Krishnan, M.; Narayan, R. Polymer 1999, 40, 3091.
14. Narayan, R.; Krishnan, M.; Snook, J. B.; Gupta, A.; DuBois, P. U.S. Pat. 5,969,089 (1999).
15. Lorcks, J. Polym Degrad Stab 1998, 59, 245.
16. Avella, M.; Errico, M. E.; Rimedio, R.; Sadocco, P. J Appl Polym Sci 2002, 83, 1432.
17. Wunderlich, B. Macromol Phys 1980, 3, 54.
18. Nielsen, L. E.; Lanel, R. F. Mechanical Properties of Polymers and Composites;, Marcel Dekker: New York, 1994; Chapter 8, p 461.
19. Wing, R. E.; Willett, J. L. Ind Crops Prod 1997, 7, 45.
20. Fllor, M.; Schenk, K. M.; Kieboom, A. P. G.; Van Bekkum, H. Starch 1989, 41, 303.
21. Parovuori, P.; Hamunen, A.; Forssell, P.; Autio, K.; Pautanen, K. Starch 1995, 47, 19.
22. Liu, X.; Wu, Q. Polymer 2001, 42, 10013.
23. Di, Y.; Lannace, S.; Di Maio, E. D.; Nicolais, L. J Polym Sci Part B: Polym Phys 2003, 41, 670.
24. Averous, L.; Fauconnier, N.; Moro, L.; Fringant, C. J Appl Polym Sci 2000, 76, 1117.
25. Nielsen, L. E.; Lanel, R. F. Mechanical Properties of Polymers and Composites; Marcel Dekker: New York, 1994; Chapter 4, p 131.
26. Massam, J.; Pinnavaia, T. J. In Material Research Society Symposium Proceedings; 1998; Beaucage, G.; Mark, J. E.; Burns, G.; Duen-Wu, H.; Eds.; 1998, 223.
27. Bajaj, P.; Jha, N. K.; Ananda Kumar, R. J. J Appl Polym Sci 1990, 40, 203.
28. Gray, R. W.; McCrum, N. G. J Polym Sci 1969, 7, 1329.
29. Nielsen, L. E. Trans Soc Rheol 1969, 13, 141.
30. Becker, O.; Varley, R.; Simon, G. Polymer 2002, 43, 4365.
31. Lin, M. S.; Lee, S. T. Polymer 1997, 38, 53.
32. Jimenez, G.; Ogata, N.; Kawai, H.; Ogihara, T. J Appl Polym Sci 1997, 64, 2211.